Two-color quantum-well infrared photodetector with voltage tunable peaks

Amlan Majumdar[a)]
Department of Electrical Engineering, Princeton University, Princeton, New Jersey 08544

K. K. Choi
U.S. Army Research Laboratory, Adelphi, Maryland 20783

J. L. Reno
Sandia National Laboratories, Albuquerque, New Mexico 87185

L. P. Rokhinson and D. C. Tsui
Department of Electrical Engineering, Princeton University, Princeton, New Jersey 08544

(Received 8 October 2001; accepted for publication 2 November 2001)

A two-color quantum-well infrared photodetector with voltage tunable detection peaks is demonstrated. It is based on electron transfer between two asymmetric coupled quantum wells under an applied bias. At 10 K, the peak detection wavelength is 7.5 μm for positive bias when the electrons reside in one of the wells, and switches to 8.8 μm at a large negative bias when the electrons are transferred to the other well. The electron activation behavior of dark current in this detector depends on both temperature and bias. We observed two distinctive activation energies under negative bias for two different temperature regimes and only one under positive bias. The voltage tunability of the detector and the activation energy are well explained by the calculated energy levels and oscillator strengths of intersubband transitions in the structure. © *2002 American Institute of Physics.* [DOI: 10.1063/1.1447004]

An important use of two-color infrared detection is remote temperature sensing.[1,2] For this application, it is desirable to have a detector with two distinctive detection wavelengths. A two-color quantum-well infrared photodetector (QWIP) with a voltage tunable detection wavelength is useful for this purpose. It can be integrated with a time-multiplexed readout circuit to greatly simplify focal plane array production. Voltage tunable two-color QWIPs have been investigated in the past based on two different mechanisms. The first approach is based on Stark shift in asymmetric multiple QW (MQW) structures.[3–5] In these structures, the responsivity is very different for different wavelengths. This creates serious difficulties in the readout design. The second approach relies on electron transfer between coupled QWs under an applied bias.[6] This approach leads to similar responsivities for different wavelengths. The existing design, however, does not exhibit effective wavelength switching. The shorter wavelength peak of the two colors is always present for both voltage polarities.[7]

We investigated the problems related to this latter approach in detail by extracting absorption coefficient α and effective photoconductive gain g of a QWIP similar to the one used in Ref. 7.[8] We found an almost constant value of α in the 6–12 μm wavelength range that indicated inefficient electron transfer between the coupled QWs. This was attributed to insufficient potential difference between the QW pair that was separated by only a 50 Å thick barrier. The line shape of the detector was entirely determined by the line shape of g, which was found to be decreasing monotonically toward longer wavelengths for both bias polarities. The decreasing g, which is related to the smaller tunneling probability of the lower energy photoelectrons, suppresses voltage switching for longer wavelength detection. In this letter, we report the design and fabrication of a two-color QWIP based on the same electron transfer mechanism. Its peak detection wavelength can be switched between 7.5 and 8.8 μm by reversing its bias polarity at $|V_b| \geqslant 3$ V. The responsivity at both wavelengths is found to be very similar which makes this detector suitable for readout integration.

The two-color QWIP consists of 36 periods of QW pairs sandwiched between a 0.5 μm thick n^+-GaAs top contact layer (1×10^{18} cm^{-3} Si doping) and a 1.5 μm thick n^+-GaAs bottom contact layer (5×10^{17} cm^{-3} Si doping). Each period consists of a 44 Å $Al_{0.05}Ga_{0.95}As$ left QW coupled to a 44 Å GaAs right QW through a 200 Å $Al_{0.3}Ga_{0.7}As$ barrier and separated from the next set of coupled wells by a 350 Å graded $Al_xGa_{1-x}As$ barrier (x graded from 0.3 to 0.25 along the growth direction). The $Al_{0.05}Ga_{0.95}As$ wells are uniformly doped (7×10^{17} cm^{-3} Si doping) while the GaAs wells and the barriers are undoped. The entire structure is grown on a semi-insulating GaAs substrate by molecular beam epitaxy.

In this detector design, we increase the barrier between the QW pair from 50 to 200 Å to enhance electron transfer between the wells. We also use a linearly graded barrier between each unit of the MQW instead of a uniform or step barrier to improve the transport of the lower energy photoelectrons. With this graded barrier, the photoelectrons in the longer wavelength peak do not have to tunnel to escape from the wells to give rise to a photocurrent. Therefore, the use of graded barriers is essential in increasing the low energy photoconductive gain for effective wavelength switching. The use of $Al_{0.05}Ga_{0.95}As$ instead of GaAs in one of the coupled wells is also crucial. It allows the detection of longer wavelengths with the same well width while preserving the absorption oscillator strength. The selective doping of this well

a)Electronic mail: majumdar@ee.princeton.edu

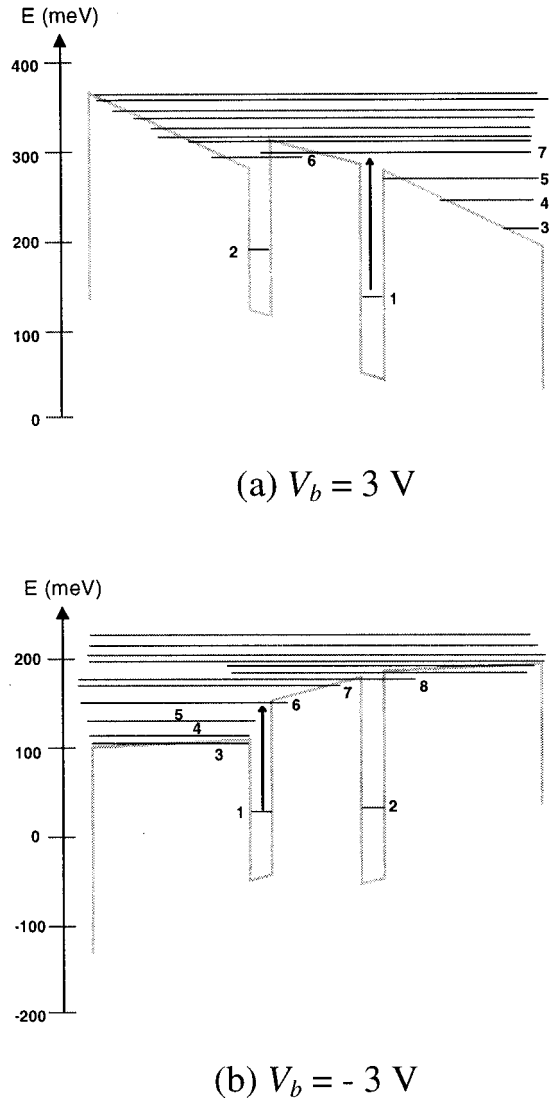

FIG. 1. Conduction band diagram and energy levels of the voltage tunable two-color QWIP for bias voltage (a) $V_b=3$ V and (b) $V_b=-3$ V. The lowest 14 levels are shown with lines. The length of these lines represents the extent of the electronic wave functions. Levels higher than 14 have been omitted because they correspond to optical transitions for $\lambda<6$ μm. The arrow indicates the intersubband transition with the largest oscillator strength: (a) $E_1\rightarrow E_7$ for $V_b=3$ V and (b) $E_1\rightarrow E_6$ for $V_b=-3$ V.

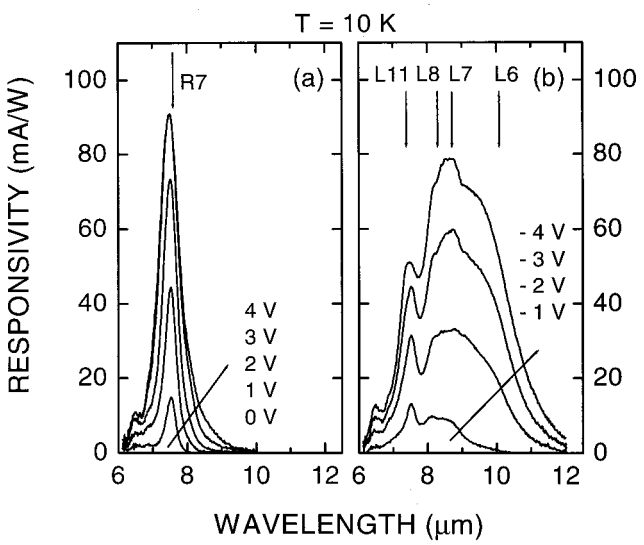

FIG. 2. Spectral responsivity R of 45°-edge coupled QWIP measured at 10 K for (a) positive and (b) negative bias. The arrows indicate calculated peak positions of intersubband transitions in the detector structure at (a) $V_b=3$ V and (b) $V_b=-3$ V. Note that the 4 V spectrum lies on top of the 3 V one for $\lambda<8$ μm and can be seen clearly for $\lambda>8$ μm.

further ensures the occupation of this well under appropriate bias.

The conduction band diagram of the QWIP structure is shown in Fig. 1 for (a) $V_b=3$ V and (b) $V_b=-3$ V. The energy scale is referenced to the right edge of the right barrier. We apply V_b to the top contact, which is on the right-hand side in Fig. 1, while keeping the bottom one grounded. The energy levels and wave functions are calculated using the transfer matrix method.[1] The lowest 14 energy levels are depicted in Fig. 1 with lines. The length of these lines represents the extent of the wave functions. For positive bias and small negative bias, the lowest energy state E_1 is in the right QW. For $V_b<-3$ V, E_1 moves to the left QW. At $V_b=-3$ V, E_1 is 4 meV below E_2 and, therefore, there are electrons in both wells.[9] For $V_b<-3.6$ V, E_1 is at least 11 meV lower than E_2 and only the left QW is occupied. We also calculated the oscillator strength of the optical transitions from the computed wave functions. At $V_b=3$ V, the largest calculated oscillator strength f is at 7.6 μm, which corresponds to the $E_1\rightarrow E_7$ transition (we call this transition R7 because E_1 is in the right QW). The next significant transition is the R10 transition at 6.5 μm with $f_{\mathrm{R10}}=0.36f_{\mathrm{R7}}$. Similarly, at $V_b=-3$ V, the $E_1\rightarrow E_6$ (L6) transition at 10.1 μm has the largest oscillator strength. Other significant transitions are L7 ($\lambda=8.7$ μm), L8 ($\lambda=8.3$ μm), and L11 ($\lambda=7.4$ μm) with $f=65\%$, 20%, and 20% of f_{L6}, respectively. Figure 1 also shows that all of these transitions are bound-to-extended transitions, and hence, should have comparable photoconductive gain.

We processed 45°-edge coupled QWIPs for responsivity and dark current measurements. 200 μm×200 μm mesas were defined by photolithography and wet etching. A 1500 Å thick layer of AuGe alloy was evaporated and then alloyed in a rapid thermal annealer at 420 °C for 5 s to form ohmic contacts to the top and bottom n^+-GaAs layers. 45°-edges were then polished on the samples to couple infrared radiation to the intersubband transitions in the MQWs.

We measured ac spectral photoresponse at 10 K in the wavelength range 6–12 μm. We show the responsivity R spectra of a typical detector in Fig. 2. For positive bias, the peak detection wavelength λ_p is 7.5 μm, close to the designed value of R7 at 7.6 μm. The linewidth $\Delta\lambda$, defined as the full width at half-maxima, is 0.6 μm. The cutoff wavelength λ_c, defined at half-maximum, is 7.8 μm. There is also a small peak at 6.5 μm, which can be assigned to the R10 transition. The peak responsivity $R(\lambda_p)$ increases with V_b till 3V, stays constant in the range 3–4 V, and then decreases for $V_b>4$ V.

Under negative bias, there is a narrow responsivity peak at 7.5 μm and a broad peak centered around 8.5 μm at $V_b=-1$ V. With increasing $|V_b|$, the size of the long wavelength peak increases more than that of the short wavelength peak as electrons are transferred to the left well. For $V_b\leqslant-2$ V, the dominant peak switches to 8.8 μm with a broad line-

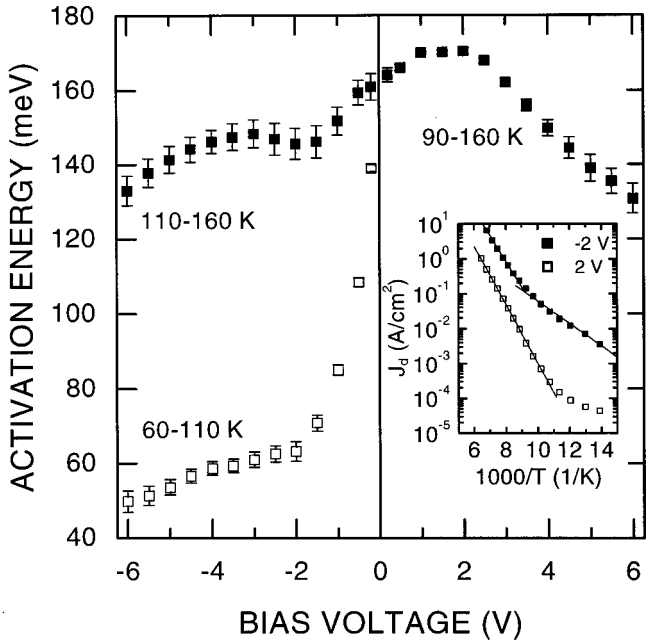

FIG. 3. Bias V_b dependence of electron activation energy E_a. Inset: Arrhenius plot of dark current density J_d for $V_b=2$ and -2 V. Symbols: experimental data, lines: least-squares fit of $J_d=J_{d0}\exp(-E_a/k_BT)$ to the data to obtain E_a. The -2 V data have been shifted up by one decade for clarity.

width of 3.5 μm. The cutoff wavelength in this case extends to 10.5 μm. The broadband response under this bias is due to absorption from the close-by transitions L6, L7, L8, and L11, as indicated in Fig. 2(b), modified by the respective gains. For this detector, switching the bias polarity at $|V_b|\geqslant 3$ V leads to a 1.3 μm shift in λ_p and a 2.7 μm change in λ_c. This clearly demonstrates the voltage tunability of the two-color detector.

It is interesting to note that this two-color detector has a short-circuit photocurrent at zero bias peaked at 7.5 μm. The peak size is 20% of the peak value at 3 V. This photovoltaic behavior of the detector arises from the presence of a built-in electric field in the graded barrier regions at zero bias.[4] Note that since E_2 is 24 meV higher than E_1 at zero bias, the energy difference is larger than E_F of 11 meV. The left QW is therefore not populated, which explains the absence of the photovoltaic effect in the long wavelength range.

We extracted the electron activation energy E_a of the QWIP dark current. The Arrhenius plot of dark current density J_d is shown in the inset of Fig. 3 for $V_b=2$ and -2 V (symbols). We fit $J_d=J_{d0}\exp(-E_a/k_BT)$ to the data to obtain E_a, where J_{d0} is a prefactor and k_B is the Boltzmann constant. The least-squares fit of this equation to the data is shown in the inset of Fig. 3. The bias dependence of the deduced values of E_a is plotted in Fig. 3. We find two different values of E_a for negative bias in two different temperature regimes: 60–110 K and 110-160 K, but only one E_a for positive bias in the 90–160 K range. For $V_b<0$, E_a in the lower T range is smaller than that in the higher T range.

The activation energy data can be understood in terms of a simple model for dark current transport. Under positive bias when only the right QW is populated, thermionic emission of electrons from E_1 to E_7 will give $E_a=E_7-E_1-E_F=300-138-11=151$ meV at 3 V.[10] This value is very close to the observed value of 162 meV. It is evident from Fig. 1(a) that thermionic emission from the left QW via thermal population of E_2 has far larger activation energy, and thus is not observed. In general, E_a decreases with V_b because of the existence of thermally assisted tunneling current. On the other hand, under negative bias, both wells are populated, and each has its own activation energy. At a low T, thermionic emission from the left QW dominates the current flow. Therefore, a smaller value of $E_a=E_3-E_1-E_F=68.5$ meV is expected at -3 V, which is consistent with the observed value of 61 meV. At high T, thermal activation in the right well becomes appreciable, and can contribute significantly to the total current. Figure 1(b) shows the thermal electrons from the right well can acquire much larger drift velocity than those from the left well due to the much larger potential drop, and hence larger electric field, in the adjacent barrier on the left. Therefore, at high T ($T>110$ K, the thermionic current from the right well can be dominant and a larger $E_a=E_8-E_2-E_F=143$ meV is expected, which is in excellent agreement with the observed value of 148 meV.

In summary, we have fabricated a voltage tunable two-color QWIP based on the transfer of electrons between coupled QWs under an applied bias. At 10 K, the peak detection wavelength is 7.5 μm for $V_b\geqslant -1$ V, shifts to 8.8 μm for $V_b\leqslant -2$ V, and therefore, can be switched between these values by reversing the bias polarity at $|V_b|\geqslant 3$ V. We found different values of electron activation energy in different temperature and bias regimes. Both wavelength switching and activation energies are well understood from the theoretical calculation of the energy levels and oscillator strengths of transitions in this QWIP structure.

The work at Princeton University is supported by the Army Research Office and the National Science Foundation. Sandia is a multiprogram laboratory operated by Sandia Corporation, a Lockheed Martin Company, for the United States Department of Energy under Contract No. DE-AC04-94 AL85000.

[1] K. K. Choi, *The Physics of Quantum Well Infrared Photodetectors* (World Scientific, River Edge, NJ, 1997).
[2] C. J. Chen, K. K. Choi, W. H. Chang, and D. C. Tsui, Appl. Phys. Lett. **72**, 7 (1998).
[3] K. K. Choi, B. F. Levine, C. G. Bethea, J. Walker, and R. J. Malik, Phys. Rev. B **39**, 8029 (1989).
[4] B. F. Levine, C. G. Bethea, V. O. Shen, and R. J. Malik, Appl. Phys. Lett. **57**, 383 (1990).
[5] E. Martinet, F. Luc, E. Rosencher, P. Bois, and S. Delaitre, Appl. Phys. Lett. **60**, 895 (1992); E. Martinet, E. Rosencher, F. Luc, P. Bois, E. Costard, and S. Delaitre, *ibid.* **61**, 246 (1992).
[6] K. K. Choi, B. F. Levine, C. G. Bethea, J. Walker, and R. J. Malik, Appl. Phys. Lett. **52**, 1979 (1988).
[7] V. Berger, N. Vodjdani, P. Bois, B. Vinter, and S. Delaitre, Appl. Phys. Lett. **61**, 1898 (1992).
[8] A. Majumdar, K. K. Choi, L. P. Rokhinson, and D. C. Tsui, Applied Physics Letters (in press).
[9] The 44 Å LQW has 7×10^{17} cm^{-3} Si doping giving a two-dimensional electron density $n_{2D}=3.1\times10^{11}$ cm^{-2}. At low temperatures, when the lowest energy level is the only occupied state, the Fermi energy $E_F=11$ meV measured from level 1. This is the case in our structure for $V_b>0$ and $V_b<-3.6$ when the level 2 is at least 11 meV higher than level 1. At $V_b=-3$ V, $E_2-E_1=4$ meV. Therefore, both subbands are occupied and $E_F=7.5$ meV.
[10] B. F. Levine, C. G. Bethea, G. Hasnain, V. O. Shen, E. Pelve, R. R. Abbott, and S. J. Hsieh, Appl. Phys. Lett. **56**, 851 (1990).